DISPERSED PASSIVE RF-SENSING FOR 3D STRUCTURAL HEALTH MONITORING

Abeer Ahmad[2], Xiao Sha[1], Akshay Athalye[1], Samir R. Das[2], Kelly Caylor[3], Branko Glišić[4], Milutin Stanaćević[1], Petar M. Djurić[1]
[1]Electrical and Computer Engineering, Stony Brook University, Stony Brook, NY 11794, [2]Computer Science, Stony Brook University, Stony Brook, NY 11794, [3]Department of Geography, UC Santa Barbara, Santa Barbara, CA 93106, [4]Civil and Environmental Engineering, Princeton University, Princeton, NJ 08544,

NOTE: Corresponding author: Petar M. Djurić, petar.djuric@stonybrook.edu

Abstract – *We propose a sensing system comprising a large network of tiny, battery-less, Radio Frequency(RF)-powered sensors that use backscatter communication. The sensors use an entirely passive technique to 'sense' the parameters of the wireless channel between themselves. Since the material properties influence RF channels, this fine-grain sensing can uncover multiple material properties both at a large scale and fine spatial resolution. In this paper, we study the feasibility of the proposed passive technique for monitoring parameters of material in which the sensors are embedded. We performed a set of experiments where the sensor-to-sensor wireless channel parameters are well-defined using physics-based modeling, and we compared the theoretical and experimentally obtained values. For some material parameters of interest, like humidity or strain, the relationship with the observed wireless channel parameters have to be modeled relying on data-driven approaches. The initial experiments show an observable difference in the sensor-to-sensor channel phase with variation in the applied weights.*

Keywords – Backscatter-based communication, battery-less tags, Internet of Things, structural health monitoring

1. INTRODUCTION

Our modern society depends critically on the sound and steadfast functioning of a variety of engineering structures, such as bridges, buildings, pipelines, geotechnical structures, aircrafts, wind turbines, and industrial facilities [1, 2]. This leads to an increasing need for accurate and reliable structural health monitoring for safety, security and performance reasons. The approaches to addressing these needs should be low cost, pervasive, scalable, low power, high resolution and suitable to being deployed for long durations of time [3, 4, 5, 6, 7, 8]. Existing approaches offer discrete and widely spaced (sparse) sensors such as strain gauges, vibrating wires, accelerometers, and discrete fiber optic sensors. These sensors neither allow reliable and accurate early detection of anomalies (damage or deterioration) at locations at even modest distances from the sensor locations, nor can they provide advanced condition monitoring functionality such as localization and quantification of damages [9]. Distributed fiber optic sensors feature improved spatial resolution but face the same challenges as discrete sensors in the cases where damage is not in a direct contact or in the proximity of sensors [10]. These sensing modalities require batteries to operate and are not amenable to automated distributed measurements with fine spatial resolution over long periods of time [10, 11].

To alleviate these caveats, wireless sensor nodes integrating discrete sensors and operating with ambient energy harvesting have been developed [11, 12]. However, the discrete sensing modalities that are amenable to ultra-low power operation are limited to temperature and capacitive sensing [13]. A promising alternative is passive RF-sensing [14]. The sensing is based on remotely monitoring Electromagnetic (EM) signature of a customized antenna [15, 16, 17, 18] or an antenna couple [19, 20] located typically on the surface or embedded in the structure. The readout device convention-

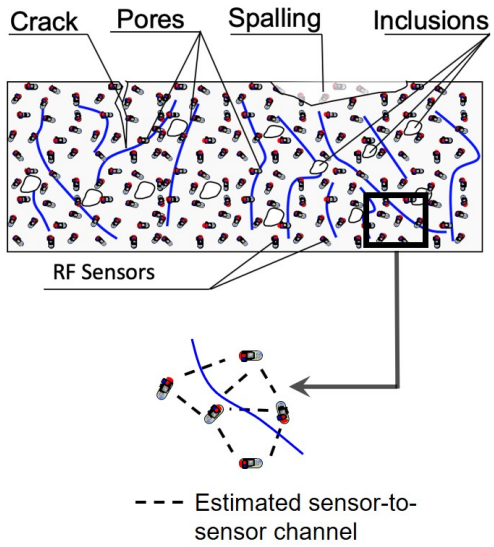

Fig. 1 – A sensing system for structural health monitoring comprising a number of RF sensors embedded in a concrete structure.

ally used is a Radio Frequency Identification (RFID) reader [21]. The deployment of costly RFID readers, however, limits the scalability of this approach [22, 23, 24, 25, 26]. Additionally, the granularity of this solution in such a centralized system is limited by the number of wireless reader-to-tag channels.

Channel estimation is a well established technique for improving the performance of a wireless communication link [27, 28]. It also enables monitoring of the environment in the vicinity of the wireless channel. RF sensors with active radio could provide granularity based on sensor-to-sensor channel estimation, but the power requirement for an active radio prohibits self-powered operation of such sensors [29].

The RF tag technology bears some similarity to conventional RFID systems that also use battery-free tags communicating via backscattering [30, 31, 32]. The RF tags can communicate among themselves, form a self-organizing network autonomously without the presence of readers. The signal that is backscattered comes from an external source, either ambient or intentionally deployed exciter(s). This signal also powers the tags, which use RF power harvesting techniques. Our recent work has extended tag-to-tag backscatter communication to RF-based sensing making the tags behave like RF sensors [33, 34, 35]. While we have demonstrated that this technique for passive wireless channel estimation can be used for activity recognition [33], here we study the feasibility of applying this method in monitoring structures in which the sensors are embedded [36].

Structural health monitoring in the proposed system is enabled by an innovative RF-sensing system composed of a network of thousands of tiny battery-free RF sensors, as illustrated in Fig. 1. The sensors are randomly distributed in the structure (both permanently embedded inside concrete and also installed on the surface). They carry out local estimation of the RF communication channels with their neighbors, with the estimates containing information about strain, temperature, humidity, and cracks. In this paper, we performed a set of experiments where the channel parameters could be obtained using physics-based modeling and compared the theoretical and experimentally obtained values. We also demonstrate a response in the phase measurement to the variation in a single material property strain.

2. BACKSCATTERING-BASED RF SENSOR AND PASSIVE CHANNEL ESTIMATION

2.1 Backscattering-based RF sensor

The enabling technology for the implementation of the proposed method, self-powered RF sensors, is based on the backscattering communication paradigm. An initial

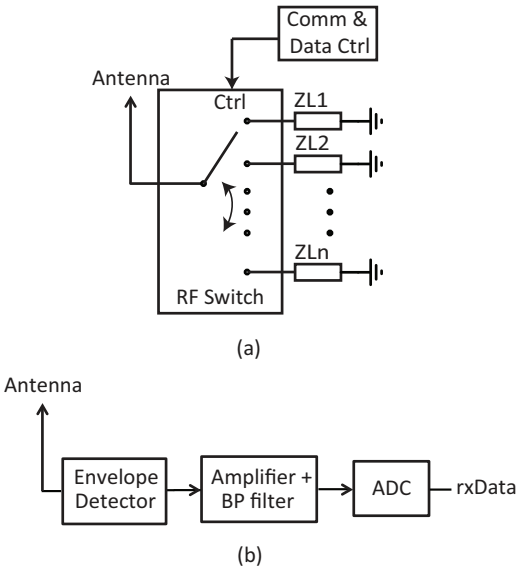

Fig. 2 – An architecture of an RF sensor, (a) a multi-phase modulator and (b) an envelope detector-based demodulator.

embodiment of this paradigm is found in RFID technology, where an RFID tag has a similar architecture to the proposed RF sensor [37]. An RFID tag comprises a modulator and a demodulator that establishes a communication link with an RFID reader. The modulator enables the RFID tag to reflect the incident RF signal at different phases. The phase is set by the terminating impedance of the antenna circuit. The modulated signal is received by the RFID reader. The RFID tag implements a demodulator based on envelope detection and resolves a modulated Continuous Wave (CW) signal emitted by the RFID reader. On the side of the RFID tag, this implementation of the modulation and demodulation leads to ultra-low power operation. At this power level, the RF sensor can harvest from the incident RF energy for its operation. However, the cost of RFID readers and the centralized system pose significant limits to deployment and resolution of these systems.

The backscattering-based RF tags eliminate the need for an RFID reader and can communicate with each other in the presence of a CW signal. Firstly, the RF tag integrates a multi-phase modulator to alleviate phase cancellation that appears in the passive communication link [38]. Secondly, amplification and filtering of the envelope signal in the demodulator enable the RF tags to resolve a modulated RF signal by another RF tag that has a low modulation index [34]. The CW signal can be an ambient RF signal or can be generated by a dedicated exciter. To translate the RF tags to sensors that can passively estimate the wireless channel, the demodulator of the RF sensor integrates an Analog-to-Digital Converter (ADC) and digitizes the processed envelope signal. The architecture of the modulator and demodulator of the RF sensor is shown in Fig. 2. In addition to the modulator and demodulator, the RF sensor inte-

grates an RF harvesting circuit that provides the voltage supply and digital control logic.

Our proposed IC implementation of the modulator and demodulator designed in the 65 nm CMOS fabrication technology consumes power lower than 1 μW [34]. This means that the power budget for the sensor that can communicate with other sensors and measure the sensor-to-sensor channel can be as low as 2 μW depending on the power of the control and computational logic. Such power can be harvested instantaneously from the input RF power on the order of -25 dBm. This leads to the autonomous operation of the RF sensor solely on harvested energy, eliminating the need for batteries as a power source.

2.2 Passive channel estimation

We present a signal-level analysis of the sensor-to-sensor channel in the presence of a dedicated exciter as a CW signal generator. The signals received at the two RF sensors, along with their respective reflection coefficients are illustrated in Fig. 3. In the analysis, we assume that the environment is static.

We first observe the signal at sensor b when sensor a is modulating it's reflection coefficient. The input RF signal at sensor b is a combination of a direct-path signal from the exciter and the signal that is first reflected of sensor a before reaching sensor b. We denote the amplitudes of the direct path channels *exciter* $\rightarrow$ *sensor* a and *exciter* $\rightarrow$ *sensor* b as A_{Ea} and A_{Eb}, respectively, while the phases are denoted as θ_{Ea} and θ_{Eb}. As the sensors integrate envelope detector as a receiver, the baseband signal represents the amplitude of the received RF signal. When the modulator of sensor a is terminated with 50 Ω, half of the input RF signal at sensor a is reflected. This termination at sensor a provides the baseline in the baseband signal at sensor b and is labeled as $\hat{v}_{b,0}$. We assume that the reflection coefficient at sensor a is further modulated with unity gain with the only change in the phase of the reflection coefficient. For the phase of the reflection coefficient, $\phi_{a,k}$, the baseband signal at the sensor b is denoted as $\hat{v}_{b,k}$. The difference between these two baseband signals at sensor b is

$$\hat{v}_{b,k} - \hat{v}_{b,0} = A_{Ea}A_{ab}\cos(\theta_{Ea} + \theta_{ab} + \phi_{a,k} - \theta_{Eb}), \quad (1)$$

where A_{ab} denotes the amplitude of the channel *sensor* $a \rightarrow$ *sensor* b and θ_{ab} is the phase [33]. These two parameters characterize the sensor-to-sensor channel and are independent of the location of the CW signal generator. The $\phi_{a,k}$ is deterministic and fixed by the sensor a modulator. Based on *(1)*, we can perform the following estimation. We vary the reflection phase of sensor a, $\phi_{a,k}$, in a span from $-\pi$ to π n times, and record $\hat{v}_{b,k}$-$\hat{v}_{b,0}$ at sensor b for each phase. From the n equations, using the least-squares method, we obtain estimates of the product of amplitudes $A_{Ea}A_{ab}$ and phase $\theta_{ab,est} = -\theta_{Ea} - \theta_{ab} + \theta_{Eb}$.

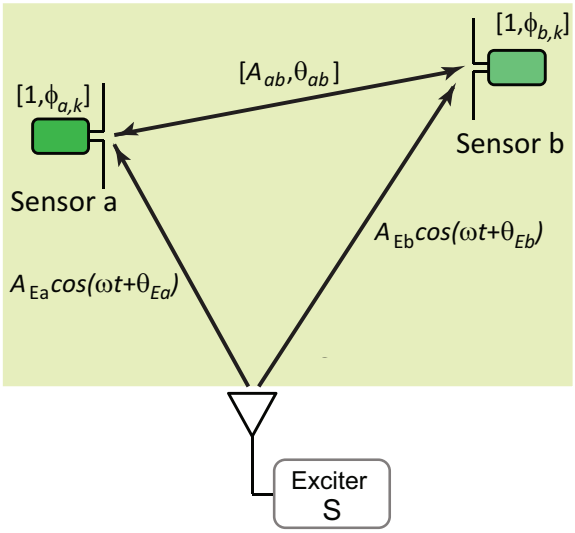

Fig. 3 – Passive estimation of the amplitude and phase, $[A_{ab},\theta_{ab}]$, of a sensor-to-sensor channel.

In order to obtain the estimates of the amplitude and channel of the sensor-to-sensor channel, we repeat the same procedure with reverse roles. Sensor b serves as modulator and the baseband signal is recorded at sensor a. The received signal at sensor a, $\hat{v}_{a,k}$, for a reflection phase $\phi_{b,k}$ is obtained similarly to *(1)*. i.e.,

$$\hat{v}_{a,k} - \hat{v}_{a,0} = A_{Eb}A_{ab}\cos(\theta_{Eb} + \theta_{ab} + \phi_{b,k} - \theta_{Ea}). \quad (2)$$

From n sampled voltages at sensor a, we obtain the estimate of the amplitude $A_{Eb}A_{ab}$ and phase $\theta_{ba,est} = -\theta_{Eb} - \theta_{ab} + \theta_{Ea}$.

Combining the estimated values for two directions of the channel, we eliminate the phases of the direct-path channel from the exciter and isolate the phase of the sensor-to-sensor channel, and we write

$$\theta_{ab,est} = -(\theta_{ab,est} + \theta_{ba,est})/2. \quad (3)$$

The estimated sensor-to-sensor channel phase is independent of the location of the exciter. This alleviates one of the critical issues for the use of other passive RF-sensing methods in structural health monitoring, as the RF sensors and the exciter/reader are located in different mediums. To obtain the estimate of A_{ab}, we have also to estimate the amplitudes of the direct-path exciter-to-sensor channel, A_{Ea} and A_{Eb}. However, the phase estimate is conventionally more robust in applications like distance measurement and localization [39].

3. SENSING OF MATERIAL PROPERTIES

We envision that the proposed RF sensors can be mixed with binding structural materials (e.g., cement, geopolymers, resins and plastic composites), or dispersed in the media (e.g., soil). Then, they could be used to evaluate

and monitor material properties at the macro-level such as integrity (presence of cracks and their propagation over time), internal humidity (water content in pores and its variability over time), strain and temperature.

It is critical to determine the imprints of the changes in material properties from the signals exchanged by the RF sensors. We first explore the relationships between the parameters of the RF channel and the material properties and/or their changes. The unwrapped version of the sensor-to-sensor channel phase θ_{ab} is obtained from the propagation model of the RF wave [37]

$$\theta_{ab,est} = \pi \frac{d}{v} f - \pi k, \qquad (4)$$

where $k \in \mathbb{Z}^+$ to keep θ_{ab} within the range 0 to π. The phase unwrapping in the sensor-to-sensor channel has a period of π, as the channel phase is a sum of two estimated phases in *(3)*. The symbol d is the distance between the sensors, and v is the velocity of the EM wave in the material. The velocity is a function of the electromagnetic parameters (permittivity and permeability) of the material that surrounds the sensors [40]. This enables indirect measurement of the material properties. It is important to note that the electromagnetic parameters of the medium are differently affected by factors like humidity and temperature at different transmission frequencies. The use of different transmission frequencies provides a larger set of independent observations in terms of the measured channel phases, leading to a more robust estimation of the material properties.

For deployment of the proposed sensors in a real-world scenario, intrinsic relationships between the parameters of interest, like humidity or strain, and the observed wireless channel, have to be modeled. Data analysis can include both physics-based and data-driven (machine learning) approaches. The modeling can be performed through numerous tests in strictly controlled conditions with a set of different parameters, distance between RF sensors, depth in material, and exciting frequency. As a first step, to demonstrate the feasibility of the proposed approach, we first study the relationship between the integrity and strain of a material. While we control only a single parameter in these experiments, we recognize that in real-world settings this is not the case and all parameters can change simultaneously leading to more complex testing and modeling.

To perform the tests that demonstrate the feasibility of the approach, the RF sensor is embedded in sand. Sand is appropriate material for exploratory tests as, typically, it has similar characteristics as concrete, a most common binding material used in engineered structures. Both relative permittivity (3-6 in dry sand vs. 6-8 in concrete) and velocity of electromagnetic waves (120-170 mm/ns in dry sand vs. 55-112 mm/ns in concrete) have similar values. Using sand instead of concrete also reduces the costs of tests, as the RF sensors can be retrieved and reused after each test.

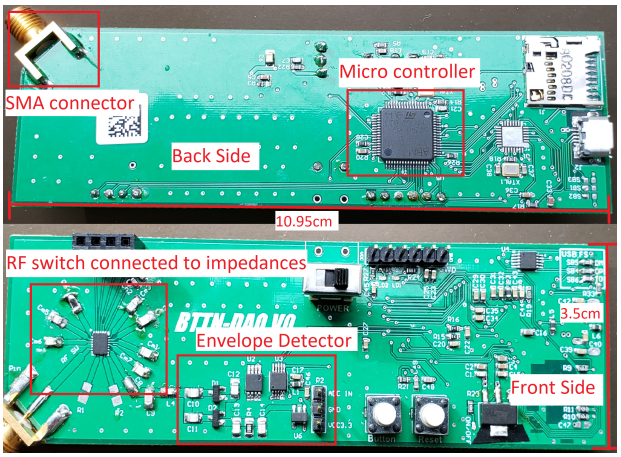

Fig. 4 – Discrete implementation of an RF sensor used in the experiments.

4. RF SENSOR IMPLEMENTATION

The RF sensor is implemented using discrete components on a Printed Circuit Board (PCB). The front and back side of the PCB, which interfaces a dipole antenna, are shown in Fig. 4. The multi-phase modulator integrates a 10-channel RF switch (SKY13404). The channels of the switch are terminated with seven impedances, which in addition to an open-circuit terminal, enable 8-phase channel estimation. The phases are preselected so that they are evenly spaced in a range of 2π with a reflection coefficient close to unity. The demodulator is based on an envelope detector, which is implemented as a two-stage Dickson rectifier with Schottky diodes, SMS7630. The envelope detector is followed by a low-pass filter and a 16-bit 1 MSample/s Analog-to-Digital Converter (ADC) ADS8860. A Microcontroller Unit (MCU), STM32F205RET6, is utilized to implement the digital control logic. The MCU communicates with the ADC chip via SPI communication and transfers the amplitude of the input RF signal to a PC through a USB connection for data analysis. As the implemented RF sensor is used as the data logger, the voltage supply to the board is supplied through a USB connection.

5. EXPERIMENTAL RESULTS

To demonstrate the feasibility of the proposed method, we performed a set of experiments. First, we demonstrate how the phase of the channel depends on the distance between tags in two different mediums. In the second set of experiments, we study the relationship between the integrity and strain of a material on the phase of the wireless channel. In our study the material is sand.

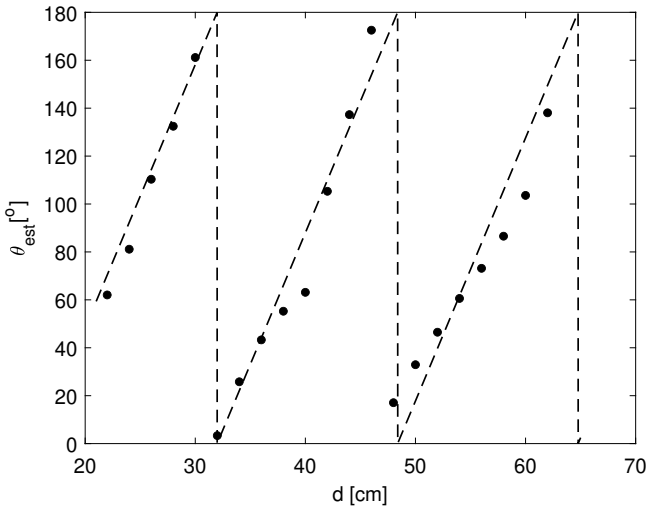

Fig. 5 – Phase of the channel in air as a function of distance between the sensors.

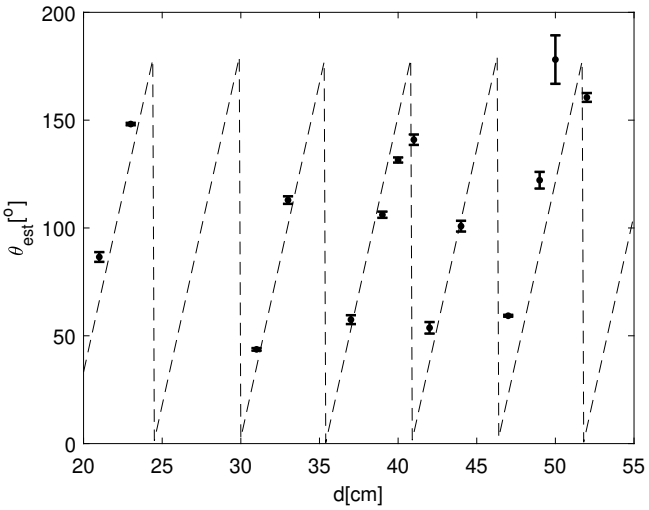

Fig. 6 – Measured phase of the sensor-to-sensor channel as a function of distance between the sensors when the sensors are buried in sand.

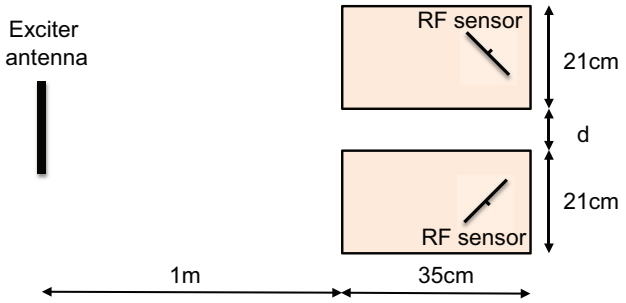

Fig. 7 – The experimental setup for the variation of air gap between the sensors.

5.1 Distance measurements for different mediums

The phase of the wireless channel was first measured as a function of the distance between the sensors in air as the medium between the sensors. The source generator was connected to a circularly polarized antenna providing CW signal at 915 MHz. The exciter antenna was positioned at distances of 2 m from the sensors, with the incident RF power at both sensors kept in the range from -20 dBm and -15 dBm during the experiment. The RF sensors described in Section 4 were positioned on a rail, and the distance was changed from 22 cm to 80 cm. For each position, each sensor modulated the reflection phase through the 8 values, and the digitized envelope signal on the opposing sensor was recorded on a PC for each phase. The estimated channel phase was computed on a PC. The plot of the phase as a function of distance between the sensors is shown in Fig. 5. The dashed line shows the ideal phase based on the velocity of the RF wave in the air. As the distance between the tags was increased, due to the reflections in the environment, the error in the phase measurement was increased. The experiment demonstrates that the phase between the tags is only a function of the sensor-to-sensor channel and not on the position of the excitation signal.

In the second experiment, the sand was used as the medium in which the RF sensors were placed. A storage container of size 75.5cm x 50.8cm x 44.5cm was filled with sand. The same exciter antenna was used as in the previous experiment, while the distance from the antenna to the sensors was reduced to 1 m in order to keep the same incident RF power at the sensors. The attenuation of the RF signal for the same distance between the exciter and the RF sensor was greater when the sensors were in the sand due to the difference in the velocity of RF wave in sand and air. The antennas of both sensors were buried in the sand at the depth of 10 cm. One sensor was kept at a fixed location, while the second sensor was moved so that the distance between the sensors varied from 22 cm to 55 cm. The variation of the channel phase with the distance between the sensors is shown in Fig. 6. At each distance, the envelope signal measurement was repeated 15 times and the standard deviation at each distance is shown. We note that the measurement noise, with a maximum value of 2^o, was much lower than the channel noise. The dashed line shows the ideal phase as a function of the distance when the velocity in the sand is 100 mm/ns.

5.2 Measurement of integrity and strain of material

We wanted to find the relationship of the sensor-to-sensor channel and the material properties, and so we performed a set of experiments. The general set-up involved two RF sensors installed at a predefined distance, embedded in material at a predefined depth, excited with a predefined frequency, and subjected to changes of only one observed parameter. We then investigated the relationship between the test parameters (distance between RF sensors and exciting frequency), the controlled material parameter, and the properties of the wireless channel between two RF sensors. Here, we present the study of dependence of the wireless channel on the mate-

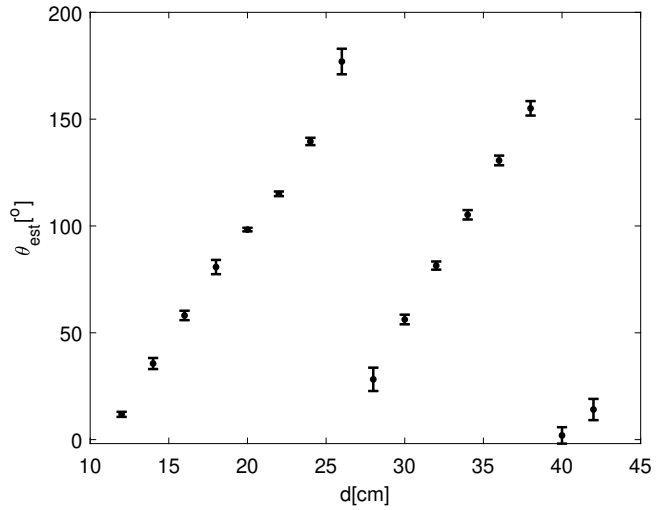

Fig. 8 – Phase of the channel in air as a function of distance between the sensors.

rial integrity and the strain. The used material in these experiments, as before, was sand.

In the first set of experiments, we controlled the air gap in the sand in order to simulate the loss of integrity in the structure, e.g., due to cracking or spalling. For precise control of the air gap, we first placed each RF sensor in a separate storage container of size 34.6cm x 21cm x 12.4cm. The storage containers were filled with sand, and the antenna of the sensor was placed at the depth of 10 cm. To simulate a different air gap, only the distance between the containers was varied, while the sensors were kept at the same location within the container, as illustrated in Fig. 7. The phase of the channel as a function of the distance between the containers, that is, air gap, is shown in Fig. 8. From the figure, we note that the wavelength of the RF wave propagation corresponds to the velocity propagation in air as expected, and the channel phase is linearly dependent on the air gap.

For a more realistic experiment, we used the experimental setup shown in Fig. 9, where air gaps are introduced in the sand. However the width of the air gap is harder to control in this case. A storage container of size 75.5cm x 50.8cm x 44.5cm was filled with sand. The sensor antennas were fixed to the opposing walls of the container where the distance between the antennas was 50 cm. The exciter antenna with circular polarization was placed at a distance of 1 m from the side of the container and at equal distance from both sensor antennas. We first measured the phase of the channel between the sensors when the container was completely filled with sand. Next, we created an air gap that was 5 cm wide in the middle of the container and measured the channel phase. The experiment was repeated with the air gap width increased by 5 cm until it became 20 cm. The phase of the channel as a function of width of the air gap is shown in Fig. 10 demonstrating changes in the phase. To demonstrate the linearity, the unwrapped phase is plotted. This large gaps do not reflect real (small) sizes of cracks in real-world settings; however, the aim of the tests was only to prove the concept.

To determine the effect of the strain on the parameters of the channel, we performed the following experiment. We used the same storage container filled with sand as in the previous experiment. The RF sensors were buried 10 cm in the sand at a distance of 50 cm. A weight of 2.3 kg was placed on top of the sand and left for 15 minutes. The weight was removed from the sand and the phase of the wireless channel was sampled every 30 seconds 15 times. After the phase measurement, a weight of 4.5 kg was placed on the top of the sand and left for 15 minutes. After removing the weight, the phase measurement was repeated in the same manner. The last weight placed on top of the sand was 6.8 kg with repeated phase measurements afterwards. The estimated channel phase as a function of the weight is presented in Fig. 11. The estimated phase shows dependence on the applied weight. However, the variance of the estimate in this set of experiments was much higher than in the previous experiments due to the settling of the sand after applying and removing the weight.

6. CONCLUSIONS

We presented RF sensors that possess a unique RF-based sensing ability; they are capable of measuring the characteristics of the intermediate wireless backscatter channel. This, in turn, gives them the ability to localize themselves and to sense environmental and material properties inside structures based on the channel characteristics they "observe." These battery-less sensors are powered by an external RF signal and operate at a near-zero power regime, which in turn enables them for a prolonged lifetime. The proposed RF sensors can be pervasively embedded and dispersed within the structural material providing the structure with self-sensing capability. These sensors will, for the first time, enable advanced structural health monitoring at high fidelity and on large scales. It will have a transformational impact on structure management and will contribute significantly to the resilience and sustainability of our society and environment.

ACKNOWLEDGEMENT

The authors are thankful for the support of NSF under Awards CNS-1763843, CNS-1901182, and CPS-2038801.

REFERENCES

[1] "Failure to act: Closing the infrastructure investment gap for America's economic future". In: *American Society of Civil Engineers* (2016).

[2] B. Glisic and D. Inaudi. *Fibre Optic Methods for Structural Health Monitoring*. Chichester, UK: John Wiley & Sons, Inc., 2007.

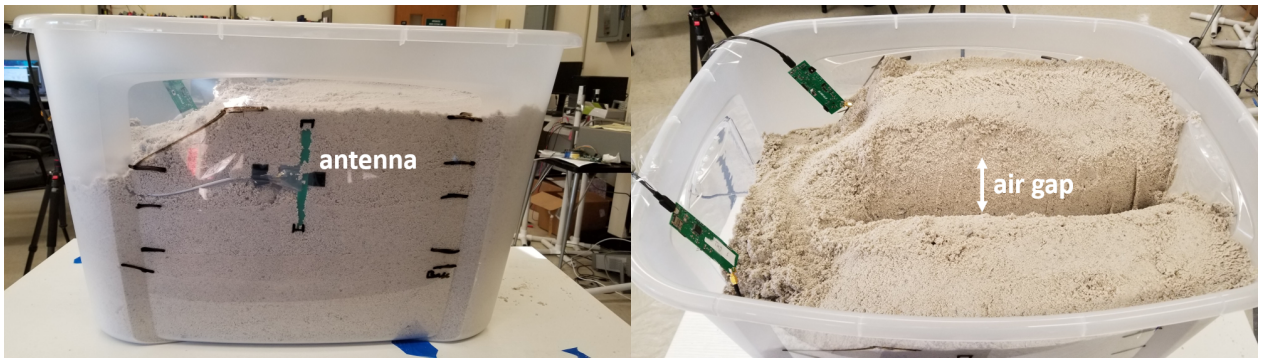

Fig. 9 – Experimental setup. Left: Side view of the antenna which is fixed to the side of the container. Right: Top view showing the air gap in the channel.

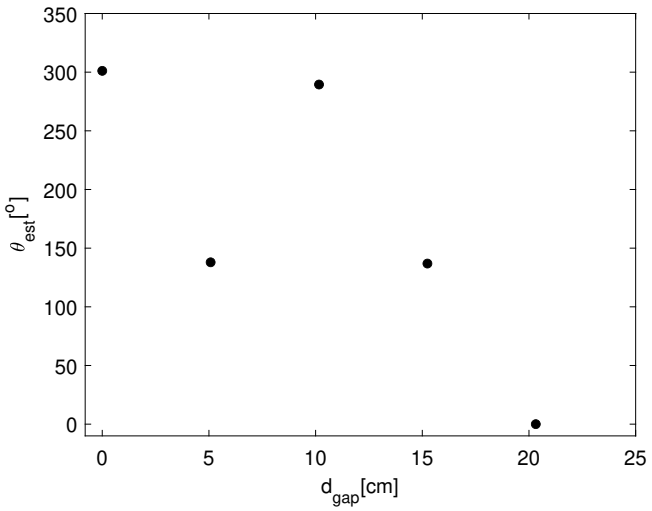

Fig. 10 – The phase of the RF sensor-to-sensor channel as a function of the air gap width created between the sensors.

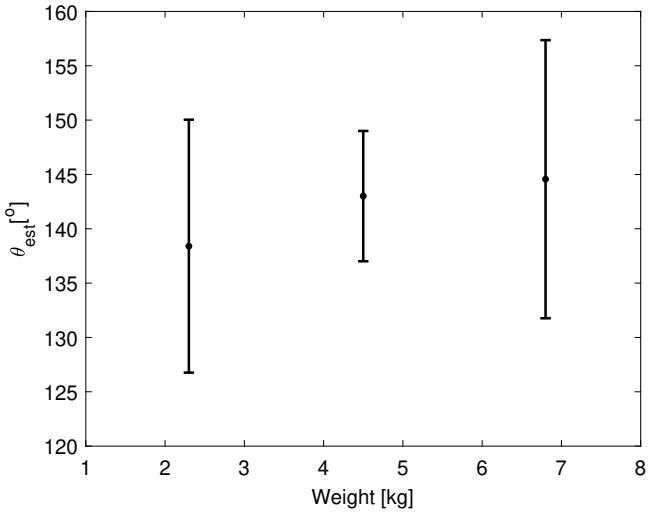

Fig. 11 – The phase of the RF sensor-to-sensor channel as a function of weight applied to the top of the sand.

[3] Daniele Zonta, Andrea Chiappini, Alessandro Chiasera, Maurizio Ferrari, Matteo Pozzi, Lorenzo Battisti, and Matteo Benedetti. "Photonic crystals for monitoring fatigue phenomena in steel structures". In: *Sensors and Smart Structures Technologies for Civil, Mechanical, and Aerospace Systems 2009*. Vol. 7292. International Society for Optics and Photonics. 2009, p. 729215.

[4] Kenneth J Loh, Tsung-Chin Hou, Jerome P Lynch, and Nicholas A Kotov. "Carbon nanotube sensing skins for spatial strain and impact damage identification". In: *Journal of Nondestructive Evaluation* 28.1 (2009), pp. 9–25.

[5] P. A. Withey, V. S. M. Vemuru, S.M. Bachilo, S. Nagarajaiah, and R.B. Weisman. "Strain paint: Noncontact strain measurement using single-walled carbon nanotube composite coatings". In: *Nano Letters* 12 (2012), pp. 3497–3500.

[6] Nathan Salowitz, Zhiqiang Guo, Sang-Jong Kim, Yu-Hung Li, Giulia Lanzara, and Fu-Kuo Chang. "Screen printed piezoceramic actuators/sensors microfabricated on organic films and stretchable networks". In: *Structural Health Monitoring* (2013), pp. 1543–1550.

[7] M. Hallaji, A. Seppänen, and M. Pour-Ghaz. "Strain paint: Noncontact strain measurement using single-walled carbon nanotube composite coatings". In: *Smart Materials and Structures* 23.8 (2014).

[8] S. Kharroub, S. Laflamme, C. Song, D. Qiao, B. Phares, and J. Li. "Strain paint: Noncontact strain measurement using single-walled carbon nanotube composite coatings". In: *Smart Materials and Structures* 24.6 (2015).

[9] Branko Glišić, Yao Yao, Shue-Ting E Tung, Sigurd Wagner, James C Sturm, and Naveen Verma. "Strain sensing sheets for structural health monitoring based on large-area electronics and integrated circuits". In: *Proceedings of the IEEE* 104.8 (2016), pp. 1513–1528.

[10] B. Glisic. “Distributed fiber optic sensing technologies and applications – an overview”. In: *ACI Special Publication* SP-292.2 (2013).

[11] Adam B Noel, Abderrazak Abdaoui, Tarek Elfouly, Mohamed Hossam Ahmed, Ahmed Badawy, and Mohamed S Shehata. “Structural health monitoring using wireless sensor networks: A comprehensive survey”. In: *IEEE Communications Surveys & Tutorials* 19.3 (2017), pp. 1403–1423.

[12] Soojin Cho, Shin Ae Jang, Hongki Jo, Kirill Mechitov, Jennifer A Rice, Hyung-Jo Jung, Chung-Bang Yun, Billie F Spencer Jr, Tomonori Nagayama, and Juwon Seo. “Structural health monitoring system of a cable-stayed bridge using a dense array of scalable smart sensor network”. In: *Sensors and Smart Structures Technologies for Civil, Mechanical, and Aerospace Systems 2010*. Vol. 7647. International Society for Optics and Photonics. 2010, p. 764707.

[13] Yoonmyung Lee, David Blaauw, and Dennis Sylvester. “Ultralow power circuit design for wireless sensor nodes for structural health monitoring”. In: *Proceedings of the IEEE* 104.8 (2016), pp. 1529–1546.

[14] Arvind Deivasigamani, Ali Daliri, C Wang, and Sabu John. “A review of passive wireless sensors for structural health monitoring”. In: *Modern Applied Science* 7.2 (2013), pp. 57–76.

[15] Prasanna Kalansuriya, Rahul Bhattacharyya, and Sanjay Sarma. “RFID tag antenna-based sensing for pervasive surface crack detection”. In: *IEEE Sensors Journal* 13.5 (2013), pp. 1564–1570.

[16] Xiaohua Yi, Chunhee Cho, James Cooper, Yang Wang, Manos M Tentzeris, and Roberto T Leon. “Passive wireless antenna sensor for strain and crack sensing—Electromagnetic modeling, simulation, and testing”. In: *Smart Materials and Structures* 22.8 (2013), p. 085009.

[17] Jun Zhang, Bei Huang, Gary Zhang, and Gui Yun Tian. “Wireless passive ultra high frequency RFID antenna sensor for surface crack monitoring and quantitative analysis”. In: *Sensors* 18.7 (2018), p. 2130.

[18] Walter D Leon-Salas and Ceki Halmen. “A RFID sensor for corrosion monitoring in concrete”. In: *IEEE Sensors Journal* 16.1 (2015), pp. 32–42.

[19] Stefano Caizzone, Emidio DiGiampaolo, and Gaetano Marrocco. “Wireless crack monitoring by stationary phase measurements from coupled RFID tags”. In: *IEEE Transactions on Antennas and Propagation* 62.12 (2014), pp. 6412–6419.

[20] Stefano Caizzone and Emidio DiGiampaolo. “Wireless passive RFID crack width sensor for structural health monitoring”. In: *IEEE Sensors Journal* 15.12 (2015), pp. 6767–6774.

[21] Jun Zhang, Gui Yun Tian, Adi MJ Marindra, Ali Imam Sunny, and Ao Bo Zhao. “A review of passive RFID tag antenna-based sensors and systems for structural health monitoring applications”. In: *Sensors* 17.2 (2017), p. 265.

[22] Sangkil Kim, Chiara Mariotti, Federico Alimenti, Paolo Mezzanotte, Apostolos Georgiadis, Ana Collado, Luca Roselli, and Manos M Tentzeris. “No battery required: Perpetual RFID-enabled wireless sensors for cognitive intelligence applications”. In: *IEEE Microwave magazine* 14.5 (2013), pp. 66–77.

[23] Alanson P Sample, Daniel J Yeager, Pauline S Powledge, Alexander V Mamishev, and Joshua R Smith. “Design of an RFID-based battery-free programmable sensing platform”. In: *IEEE Transactions on Instrumentation and Measurement* 57.11 (2008), pp. 2608–2615.

[24] D.J. Yeager, A.P. Sample, and J.R. Smith. “Wisp: A passively powered UHF RFID tag with sensing and computation”. In: *RFID Handbook: Applications, Technology, Security, and Privacy* (2008), pp. 261–278.

[25] H. Zhang, J. Gummeson, B. Ransford, and K. Fu. “Moo: A batteryless computational RFID and sensing platform”. In: *University of Massachusetts Computer Science Technical Report UM-CS-2011-020* (2011).

[26] M. Buettner, B. Greenstein, and D. Wetherall. “Dewdrop: an energy-aware runtime for computational RFID”. In: *Proc. USENIX NSDI*. 2011, pp. 197–210.

[27] Heinrich Meyr, Marc Moeneclaey, and Stefan Fechtel. *Digital Communication Receivers: Synchronization, Channel Estimation, and Signal Processing*. John Wiley & Sons, Inc., 1997.

[28] Ye Li, Nambi Seshadri, and Sirikiat Ariyavisitakul. “Channel estimation for OFDM systems with transmitter diversity in mobile wireless channels”. In: *IEEE Journal on Selected Areas in Communications* 17.3 (1999), pp. 461–471.

[29] J. Blanckenstein, J. Klaue, and H. Karl. “A Survey of Low-Power Transceivers and Their Applications”. In: *IEEE Circuits and Systems Magazine* 15.3 (2015), pp. 6–17.

[30] Vincent Liu, Aaron Parks, Vamsi Talla, Shyamnath Gollakota, David Wetherall, and Joshua R Smith. “Ambient backscatter: wireless communication out of thin air”. In: *ACM SIGCOMM Computer Communication Review*. Vol. 43. 4. ACM. 2013, pp. 39–50.

[31] Aaron N Parks, Angli Liu, Shyamnath Gollakota, and Joshua R Smith. "Turbocharging ambient backscatter communication". In: *ACM SIGCOMM Computer Communication Review*. Vol. 44. 4. ACM. 2014, pp. 619–630.

[32] Jihoon Ryoo, Jinghui Jian, Akshay Athalye, Samir R Das, and Milutin Stanaćević. "Design and evaluation of "BTTN": a backscattering tag-to-tag network". In: *IEEE Internet of Things Journal* 5.4 (2018), pp. 2844–2855.

[33] J. Ryoo, Y. Karimi, A. Athalye, M. Stanaćević, S. R. Das, and P. M. Djurić. "BARNET: Towards Activity Recognition Using Passive Backscattering Tag-to-Tag Network". In: *Proceedings of the 16th Annual International Conference on Mobile Systems, Applications, and Services*. ACM. 2018, pp. 414–427.

[34] Yasha Karimi, Yuanfei Huang, Akshay Athalye, Samir Das, Petar M. Djurić, and Milutin Stanaćević. "Passive wireless channel estimation in RF tag network". In: *2019 IEEE International Symposium on Circuits and Systems (ISCAS)*. IEEE. 2019, pp. 1–5.

[35] M Stanaćević, A Athalye, ZJ Haas, SR Das, and P. M. Djurić. "Backscatter Communications with Passive Receivers: From Fundamentals to Applications". In: *ITU Journal* 1.1 (2020).

[36] Milutin Stanaćević, Abeer Ahmad, Xiao Sha, Akshay Athalye, Samir Das, Kelly Caylor, Branko Glisić, and Petar M Djurić. "RF Backscatter-Based Sensors for Structural Health Monitoring". In: *2021 International Balkan Conference on Communications and Networking (BalkanCom)*. IEEE. 2021, pp. 71–74.

[37] Daniel M Dobkin. *The RF in RFID: UHF RFID in Practice*. Newnes, 2012.

[38] Zhe Shen, Akshay Athalye, and Petar M Djurić. "Phase cancellation in backscatter-based tag-to-tag communication systems". In: *IEEE Internet of Things Journal* 3.6 (2016), pp. 959–970.

[39] Steven M Kay. *Modern Spectral Estimation: Theory and Application*. Pearson, 1988.

[40] Rich Fletcher, Uttara P Marti, and Rich Redemske. "Study of UHF RFID signal propagation through complex media". In: *2005 IEEE Antennas and Propagation Society International Symposium*. Vol. 1. IEEE. 2005, pp. 747–750.

AUTHORS

Abeer Ahmad received a B.S. degree in electrical engineering from Lahore University of Management Sciences, Pakistan. He is currently a PhD student in the Department of Computer Science at Stony Brook University. He works on applications enabled by backscattering systems like object tracking and localization, ambient intelligence and structural health monitoring.

Xiao Sha received a bachelor's degree in physics and economics from Xi'an Jiaotong University. He is currently pursuing a Ph.D. degree in the Department of Electrical and Computer Engineering at Stony Brook University, Stony Brook, NY. His research interests include mixed-signal and RF circuit and system design.

Akshay Athalye is a co-founder of Scandent LLC, New York, NY, USA, where he currently serves as Chief Technology Officer. He is also an adjunct professor with the Department of Electrical and Computer Engineering, Stony Brook University, Stony Brook, NY, USA. He has been involved in RFID, backscatter communications and related research for more than a decade. He has received the IEEE Region 1 Technical Excellence Award.

Samir R. Das is a professor in the Department of Computer Science at Stony Brook University. His research interests are in wireless networking and mobile computing, focusing on protocols, systems and performance evaluation. He co-chaired the technical program committees of premier mobile networking conferences, including ACM MobiHoc and ACM MobiCom. He served on the editorial boards of IEEE/ACM Transactions on Networking and IEEE Transactions on Mobile Computing.

Kelly Caylor is the director of the UCSB Environmental Research Institute and holds joint appointments at the Bren School and the Department of Geography. In his research, Professor Caylor seeks to develop improved insight into the way that land use and climate change are interacting to affect the dynamics and resilience of global drylands. His primary research sites are in sub-Saharan Africa, where he is focused on understanding the vulnerability of pastoral and subsistence agricultural communities to current and future changes in hydrological dynamics. Professor Caylor conducts research at a number of spatial and temporal scales; from small-scale experiments during individual rainfall events all the way up to continental-scale analyses of climate trends. A major focus of his research is the development of new methods to improve the measurement and prediction of ecosystem water-use efficiency and novel observation networks for characterization of coupled natural-human system dynamics. Professor Caylor has served on the editorial board of Water Resources Research; the Journal of Geophysical Research — Biogeosciences; Vadose Zone Journal, and Environmental Research Reviews, Environmental Research Letters. He was a recipient of an Early Career Award from the NSF, and was the inaugural recipient of the Early Career Award in Hydrological Sciences given by the American Geophysical Union (AGU).

Branko Glišić received his degrees in civil engineering and theoretical mathematics at the University of Belgrade, Serbia, and Ph.D. at the EPFL, Switzerland. After an eight-year long experience at SMARTEC SA, Switzerland, he has been employed as an associate professor of civil and environmental engineering at Princeton University. His research focus is on universal Structural Health Monitoring (SHM) methods; emerging sensing technologies; advanced data analysis for diagnostics, prognostics, and decision-making; smart, kinetic, deployable, and adaptable structures; holistic analysis of heritage structures; and engineering and the arts in general. Prof. Glišić is author and coauthor of more than a hundred published papers, several university courses, and training courses for practitioners. He is a Council Member and fellow of ISHMII, and a member of several other professional associations and journal editorial boards. Prof. Glišić received several awards for his research and teaching.

Milutin Stanaćević received a B.S. degree in electrical engineering from the University of Belgrade, Serbia and a Ph.D. degree in electrical and computer engineering from Johns Hopkins University, Baltimore, MD. He is currently an associate professor in the Department of Electrical and Computer Engineering at Stony Brook University, Stony Brook, NY. His research interests include mixed-signal and RF circuit and system design. Dr. Stanaćević is a recipient of the National Science Foundation CAREER award.

Petar M. Djurić received B.S. and M.S. degrees in electrical engineering from the University of Belgrade, Belgrade, Yugoslavia, respectively, and a Ph.D. degree in electrical engineering from the University of Rhode Island, Kingston, RI, USA. He is a SUNY Distinguished Professor and currently a Chair of the Department of Electrical and Computer Engineering, Stony Brook University, Stony Brook, NY, USA. His research has been in the area of signal and information processing with primary interests in the theory of Monte Carlo-based methods; Bayesian machine learning; signal modeling, detection, and estimation; signal and information processing over networks; RFID and the IoT. Recently, his research has been applied to problems related to machine learning methods for intrapartum fetal monitoring and brain signals. He has been invited to lecture at many universities in the United States and overseas. Prof. Djurić was a recipient of the IEEE Signal Processing Magazine Best Paper Award in 2007 and the EURASIP Technical Achievement Award in 2012. In 2008, he was the Chair of Excellence of Universidad Carlos III de Madrid-Banco de Santander. From 2008 to 2009, he was a Distinguished Lecturer of the IEEE Signal Processing Society. He has been on numerous committees of the IEEE Signal Processing Society and of many professional conferences and workshops. He was Editor-in-Chief of the IEEE Transactions on Signal and Information Processing over Networks. Prof. Djurić is a Fellow of IEEE and EURASIP.